Int. J. High Technology Ceramics **1** (1985) 3 30

High Purity Mullite Ceramics by Reaction Sintering

P. D. D. Rodrigo* and P. Boch

ENSCI, 47 avenue Albert Thomas, 87065 Limoges Cedex, France

SUMMARY

A review of studies of the synthesis and densification of mullite ceramics suggests that reaction sintering could be the best way to obtain high purity, dense mullite from common materials (amorphous silicon dioxide and α-aluminium oxide). The use of fine grain powder mixtures allows us to obtain dense ceramics after firing at 1600°C, because such fine powders favour densification more than mullite formation, which slows down the sintering rate. The aluminium oxide to silicon dioxide ratio appears to be a critical parameter: densification reaches its maximum (97%) for the stoichiometric $3Al_2O_3 \cdot 2SiO_2$ (mullite), whereas it reaches its minimum for compositions close to 75·0 wt% Al_2O_3, in which excessive grain growth occurs. Moreover, these compositions seem to correspond to the solubility limit of Al_2O_3 in mullite.

1. INTRODUCTION

Mullite is the main crystalline phase in most of the alumino-silicate ceramics, and the Al_2O_3–SiO_2 system, to which mullite belongs, has been extensively studied. Besides, mullite is an important refractory material, which is generally produced by fusion in an electric arc furnace. However, rather few studies have been devoted to the production of high purity, dense mullite ceramics. Nevertheless, the properties of mullite can explain the growing interest that this material arouses as a potential engineering

* On leave from the Department of Materials Engineering, University of Moratuwa, Sri Lanka.

Int. J. High Technology Ceramics 0267-3762/85/$03·30

ceramic: good chemical and thermal stability, high refractoriness and low creep rate, low thermal expansion and thermal conductivity, medium strength and toughness, not very far from those of alumina, not to mention useful dielectric properties.

The present paper begins with a review of studies on the synthesis and sintering of mullite ceramics, and lists the principal data about mullite formation and mullite sintering in order to draw attention to the influence of the main parameters: the nature of the raw materials, particle size, aluminium oxide to silicon dioxide ratio, and additives or impurities. Because of the seemingly low atomic mobility in mullite, and the fact that high purity, fine grain, mullite powders are not common ceramic raw materials, we will then examine the reaction sintering of silicon dioxide and aluminium oxide mixtures, in order to determine the best way of producing high-quality mullite ceramics.

2. HIGH PURITY MULLITE CERAMICS

2.1. The Al_2O_3–SiO_2 binary system

This system appeared to be simple when the first equilibrium diagram was proposed by Bowen and Greig[1] in 1924. According to these authors, mullite is a compound of a fixed composition, $3Al_2O_3 \cdot 2SiO_2$ (71·8 wt % Al_2O_3), which melts incongruently at 1810 °C. Since then there have been many conflicting views on the Al_2O_3–SiO_2 diagram, mainly concerning mullite.

In 1962 Aramaki and Roy[2] proposed a new diagram in which mullite is a solid solution, stable in the range of composition from 71·8 to 74·3 wt % Al_2O_3, which melts congruently at 1850 °C. They provided evidence for the possibility of extending the range of mullite solid solution up to about 77·5 wt % Al_2O_3 under metastable conditions. Although this diagram is in good agreement with the results of studies demonstrating the solubility of Al_2O_3 in 3:2 mullite[3-6] and the congruent melting of mullite,[7-9] it did not explain the observed incongruent melting of mullite.[6,10-12]

Aksay and Pask[13] were the first to explain both congruent and incongruent melting of mullite. The binary system (Fig. 1), constructed using their own experimental results and those of many other workers,[2,14-20] shows that under stable equilibrium conditions mullite melts incongruently at 1828 ± 10 °C; its stable solid solution ranges from 70·5 to 74·0 wt % Al_2O_3 below 1753 °C and from 71·6 to 74·0 wt % Al_2O_3 at 1813 °C. However, they observed that ordered mullite melts congruently during superheating in the absence of α-Al_2O_3 and that disordered mullite solidifies congruently from supercooled aluminium silicate melts. These observations

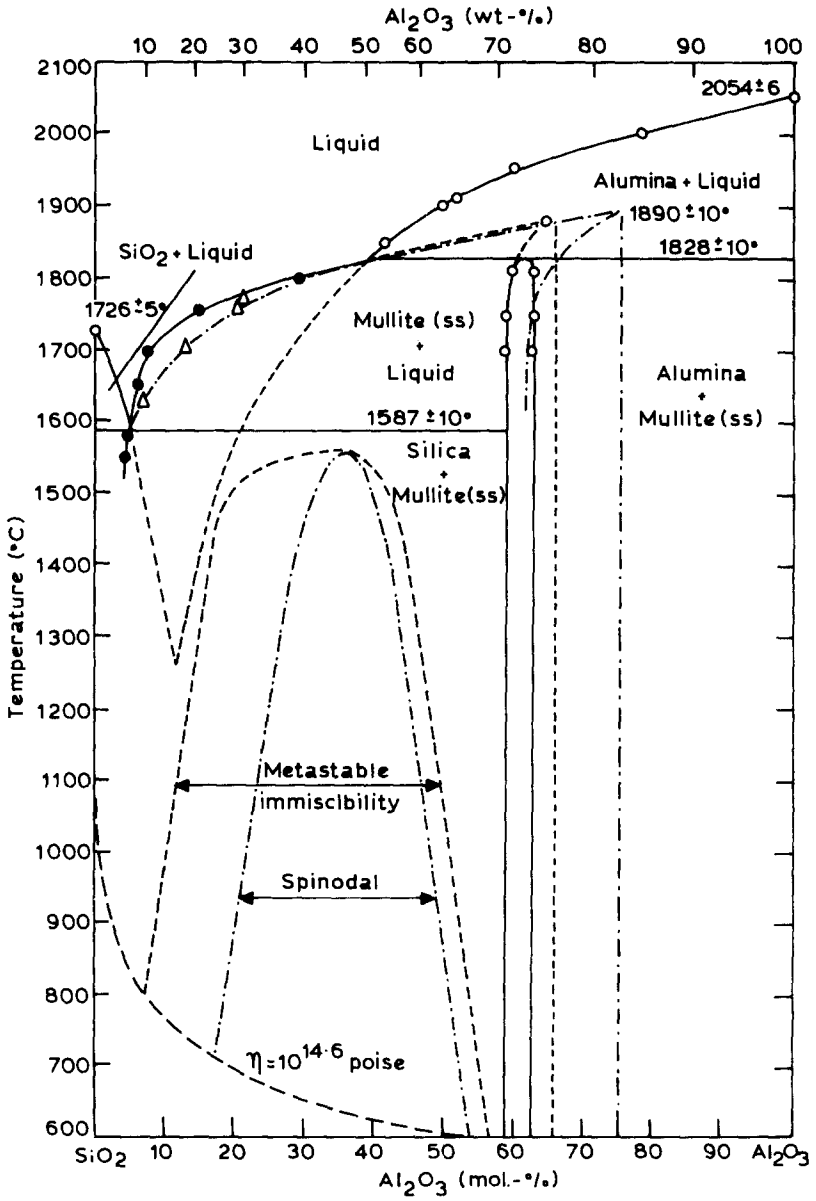

Fig. 1. The Al_2O_3-SiO_2 system according to Aksay and Pask.[13]

were shown to be associated with the difficulty of nucleation of α-Al_2O_3 in the absence of α-Al_2O_3 nuclei or nucleation sites such as sharp edges. This leads to the conclusion that congruency of mullite is observed under metastable conditions. The SiO_2-ordered mullite metastable diagram (ordered mullite melts congruently at $\simeq 1880\,°C$ and its solid solution range extends to $\simeq 77\,wt\%$ Al_2O_3) and the SiO_2-disordered mullite metastable

TABLE 1
Mullite Formation from Different Raw Materials

Reference	*Raw materials*	*Beginning of mullitization*	*Completion of mullitization*	*Other remarks*
28	Aluminium oxide–silicon dioxide mixtures prepared by hydrolysing tetraethyl silicate in the presence of aluminium hydroxide	1100–1200 °C		
29	Aluminium trichloride and silicon tetrachloride; hydroxides coprecipitated using ammonium hydroxide and dried at 150 °C	≃1100 °C	≃1150 °C	
30	Aluminium oxide–silicon dioxide mixtures of 3:2 composition prepared by hydrolysing a mixture of aluminium tris isopropoxide and silicon tetrakis isopropoxide	≃1200 °C		Surface area of as-prepared powder ≃550 $m^2 g^{-1}$ decreased down to ≃280 $m^2 g^{-1}$ when calcined at 600 °C for 1 h
27	Very fine γ-aluminium oxide (300 Å) and amorphous silicon dioxide (130–140 Å) mixed via a gel technique	≃1200 °C	≃1400 °C	
26	Aluminium oxide–silicon dioxide mixtures prepared from organo-metallic precursors	≃1200 °C	≃1500 °C	At 980 °C mixtures contained γ-Al_2O_3, HAl_5O_8 and amorphous silicon dioxide
31	Amorphous colloidal precipitate obtained from aluminium trichloride and silicon tetrachloride treated according to a process described by authors		Only mullite at 1400 °C	
36	A solution of aluminium nitrate and ethyl silicate in water–methanol (1:1 by volume) dried at 350 to 650 °C, by spraying into a reaction tube	≃980 °C	Only mullite at >980 °C	
22	α-Aluminium oxide (A14-ALCOA) and cristobalite α-Aluminium oxide (A14-ALCOA) and quartz	After 6 h at 1415 °C After 24 h at 1415 °C		Mean particle size of all powders was ≃3 μm
32	Baker's aluminium hydroxide and silicic acid		After 8 h at 1700 °C	
33	α-Aluminium oxide (A14-ALCOA) and α-quartz (Illinois Mineral Co.)		After 8 h at 1700 °C	
35	High purity aluminium oxide and quartz mixtures of 3:2 (71·8 wt% aluminium oxide) composition		≃5·5 wt% unreacted aluminium oxide after 12 days at 1500–1540 °C with four intervening grinding and mixing periods	
23	α-Aluminium oxide (XA16-ALCOA) and fused silica (Corning 7940)	≃1480 °C		
34	Aluminium oxide (KC-14, Kaiser aluminium and chemical sales) and potter's flint, mixed and ground for 48 h in a ball mill — 71·8 wt% Aluminium oxide 77·2 wt% Aluminium oxide		A very little unreacted aluminium oxide after sintering at 1710 °C A considerable amount of unreacted aluminium oxide after sintering at 1650 °C	Both mixtures contained 1 wt% magnesium oxide

diagram (disordered mullite melts congruently at $\simeq 1900\,^{\circ}C$ and its solid solution range extends to $\simeq 83{\cdot}0$ wt % Al_2O_3) correspond to two metastable conditions. In addition, the results of Davis and Pask[15] have shown the existence of a third Al_2O_3(α-Al_2O_3)–SiO_2(cristobalite) metastable diagram with a eutectic at low temperature ($\simeq 1260\,^{\circ}C$) but no mullite.

2.2. Synthesis of mullite

There have been many studies of the effects of different parameters on the synthesis of high purity mullite from aluminium oxide and silicon dioxide, or other synthetic raw materials which transform into these two oxides on heating. The crystalline form of the initial raw materials, their particle size, the SiO_2/Al_2O_3 ratio of the initial composition, and the presence of additives or impurities were found to be the major parameters controlling the mullite formation temperature and the nature of the final product.

2.2.1. Effect of the crystalline form of the SiO_2 and Al_2O_3 components
Wahl *et al.*[21] studied the formation of mullite from mixtures of α-quartz, silicic acid or β-cristobalite, with diaspore ($HAlO_2$), gibbsite ($Al(OH)_3$) or α-Al_2O_3. The mixtures of 1:4, 2:3, 3:2 and 4:1 SiO_2/Al_2O_3 mole ratio (or 87·2, 71·8, 53·1 and 29·8 wt % Al_2O_3) were prepared by mixing each of the SiO_2 components with each of the Al_2O_3 components and were fired up to 1450 °C. The X-ray diffraction experiments showed that cristobalite reacts better than the other two SiO_2 components with any of the three Al_2O_3 components and diaspore reacts better than the other two Al_2O_3 components with any of the three SiO_2 components. Their finding concerning cristobalite was later confirmed by Pask and co-workers,[22,23] who studied the sintering behaviour of the mixtures of quartz, cristobalite or amorphous silicon dioxide with α-Al_2O_3 (Table 1). Pask and co-workers explained the earlier formation of mullite in the cristobalite–α-Al_2O_3 mixture as a result of the formation of a metastable liquid phase, in accordance with the metastable Al_2O_3–cristobalite diagram without mullite. Staley and Brindley[24] have also noted the formation of such a non-crystalline phase during reactions between cristobalite and corundum and they considered it as a feature of the subsolidus reaction in the Al_2O_3–SiO_2 system.

DeKeyser[25] studied reactions occurring at 1600 °C at the interface between pressed pellets of aluminium oxide and silicon dioxide and found that a glassy phase was formed as a result of the diffusion of aluminium oxide into the silicon dioxide zone, while the mullite crystals grew with their *c*-axes oriented parallel to the direction of diffusion as a result of the movement of silicon dioxide into the aluminium oxide zone. Using DTA

results on aluminium oxide–silicon dioxide mixtures of various compositions, prepared from organo-metallic precursors, West and Gray[26] studied mullite formation up to 1500 °C, and reported that mullite develops at 1000 °C if the reaction is between amorphous silicon dioxide and hydrogen aluminium spinel (HAl_5O_8), whereas it develops at about 1200 °C once HAl_5O_8 is completely transformed into γ-Al_2O_3, which is less reactive than the defect spinel, HAl_5O_8.

Considering the crystal chemistry of the mullitization of kaolinite via metakaolinite (which has a γ-Al_2O_3-type spinel structure), Ghate *et al.*[27] assumed that γ-Al_2O_3 should react easily with amorphous silicon dioxide to give mullite. Mixtures of 71·8 wt% Al_2O_3 of amorphous silicon dioxide (130–140 Å) and γ-Al_2O_3 (300 Å), prepared by them via a gel technique, mullitized completely after 20 h at 1420 °C. The absence of α-Al_2O_3 during mullitization, and the gradual disappearance of traces of silicon dioxide, suggested the reaction was most likely occurring through diffusion and rearrangement of the spinel structural unit in agreement with the original hypothesis.

From all these data it is clear that the mullite-forming temperature is highly controlled by the crystalline forms of the SiO_2 and Al_2O_3 components. Cristobalite and γ-Al_2O_3, or other aluminium oxide components with a defect structure, seem to be the most reactive of the silicon dioxide and aluminium oxide components.

2.2.2. Effect of the particle size of aluminium oxide and silicon dioxide components

The experimental results of different investigators, summarized in Table 1, show that the mullitization of aluminium oxide–silicon dioxide mixtures has always been easier (complete mullitization below $\simeq$1500 °C) for techniques giving ultrafine particles,[26–31] whereas, in classical powder mixtures of larger particle size, detectable amounts of mullite are formed only at temperatures above 1400 °C and complete mullitization requires treatments at a temperature near 1700 °C. This is in good agreement with the generally accepted fact that the rate of a solid-state reaction increases as the particle size of the constituents decreases.

2.2.3. Effect of aluminium oxide/silicon dioxide ratio

The results of most of the investigations dealing with this subject are summarized in Table 2. None of the investigators have studied the effect of the aluminium oxide/silicon dioxide ratio on mullitization temperature. However, Wahl *et al.*[21] have observed that the beginning of mullite formation in diaspore–cristobalite mixtures always occurs at 1200 °C,

whatever the aluminium oxide/silicon dioxide ratio. This could suggest that mullitization temperature is not considerably affected by the aluminium oxide/silicon dioxide ratio.

It appears that firing silicon dioxide–aluminium oxide mixtures in the absence of a liquid phase produces mullite of nearly stoichiometric (3:2) composition (71·8 wt% Al_2O_3), though some exceptions[26] have been noticed. Probably the composition of such mullite lies in the stable solid solution range which varies from ≃70·5 to ≃74·0 wt% Al_2O_3 below ≃1750 °C (Fig. 1).

Mullites of higher aluminium oxide contents (>74·0 wt% Al_2O_3) are formed only in the presence of a liquid phase, as has been observed by Kriven and Pask,[38] Risbud and Pask,[39] and Neuhaus and Richartz[5] in supercooled aluminium silicate liquids. Such high aluminium oxide meltgrown mullites are sensitive to heat treatments, and a long annealing at a subsolidus temperature leads to exsolution of aluminium oxide.

Meltgrown mullite (or mullite formed in the presence of a liquid phase) always exhibits an acicular morphology, whereas the microstructure of mullite formed in the absence of a liquid phase can be equiaxed, and varies depending on the nature and the purity of raw materials, as well as on the composition of the starting aluminium oxide–silicon dioxide mixture. The presence of free aluminium oxide in the final product due to a high aluminium oxide/silicon dioxide ratio of the starting mixture[28,33] and/or the absence of even a small amount of intergranular glassy phase—as the one which can be formed in the presence of impurities[27]—lead to a chunky, granular microstructure. On the other hand, the choice of amorphous raw materials, intimately mixed in a molecular scale[28,30] and/or the presence of an intergranular glassy phase,[30,33] lead to a microstructure with acicular or elongated grains.

2.2.4. Effect of the presence of additives or impurities

Although this has been the subject of a large number of investigations, it is difficult to interpret the results of most of those studies, because the natural raw materials used (e.g. kaolinite) may have already contained unknown, and perhaps noticeable, amounts of different impurities. Therefore, it seems preferable to consider only the results of investigations done using high purity synthetic raw materials (Table 3).

Iron(III) oxide, chromium(III) oxide and titanium dioxide have been found to enter into solid solution with mullite in considerable quantities (respectively, 10–12 wt% above 1300 °C, 8–10 wt% above 1600 °C and 2–4 wt% above 1300 °C). They cause an increase of the unit cell volume. Because the presence of zirconium dioxide increases the sintering rate of mullite, a very low solubility of zirconium dioxide in mullite, as reported by

TABLE 2
Effect of Composition on Synthesis and Microstructure of Mullite

Reference	*Raw materials and preparation of aluminium oxide–silicon dioxide mixtures*	*Composition of the mixtures*	*Firing conditions*	*Crystalline phases present*	*Microstructural details*	*Other remarks*
21	Diaspore + cristobalite and gibbsite + silicic acid	87·18, 71·80, 53·13 and 29·82 wt% aluminium oxide	Fired up to ≃1450 °C	Mullite, corundum and cristobalite in all mixtures		Amount of mullite was always high for 71·8 wt% Al_2O_3 composition; mullitization temperature is not affected by aluminium oxide/silicon dioxide ratio
34	Aluminium oxide + potter's flint + magnesium oxide mixed and ground for 48 h in a ball mill and dried at 110 °C	71·8 wt% aluminium oxide + 1 wt% magnesium oxide	Fired up to 1710 °C	Almost 100% mullite		A mechanical mixture of fired 71·8 wt% Al_2O_3 composition and corundum with a total of 77·2 wt% Al_2O_3 gave an XRD pattern similar to that of fired 77·2 wt% Al_2O_3 composition
		77·2 wt% aluminium oxide + 1 wt% magnesium oxide	Fired up to 1650 °C	Mullite and corundum		
37	Amorphous silicon dioxide and amorphous aluminium oxide	71·8 wt% aluminium oxide	Fired at 1690 °C for 8 h	Only mullite		
29	Aluminium trichloride and silicon tetrachloride; hydroxides coprecipitated using ammonium hydroxide and dried at 150 °C	62·96 wt% aluminium oxide	Fired up to 1500 °C	Mullite and cristobalite		
		68·00, 71·83 and 74·84 wt% aluminium oxide		Only mullite		
		77·27 wt% aluminium oxide		Mullite and corundum		
33	γ-Aluminium oxide (A14-ALCOA) and γ-quartz wet mixed in a porcelain ball mill, dried and calcined at 1700 °C for 8 h	60·0 and 65·0 wt% aluminium oxide	Sintered at 1700 °C	Mullite	Totally densified due to the presence of a large amount of liquid phase	
		71·8, 73·0 and 74·0 wt% aluminium oxide	Sintered at 1700 °C	Mullite	A very small amount of an intergranular glassy phase led to the formation of a few elongated grains in an equiaxed matrix	
		75·0, 80·0, 85·0 and 90·0 wt% aluminium oxide	Sintered at 1700 °C	Mullite and corundum	Mullite and corundum formed an equiaxed structure	
36	A solution of aluminium nitrate and ethyl silicate in water–methanol (1:1 by volume), spray dried at 350–650 °C	71·8 wt% aluminium oxide	Calcined up to 1000 °C and sintered at 1650 °C for 4 h	Only mullite at any temperature above 980 °C		

28	Hydrolysing tetraethyl silicate in the presence of aluminium hydroxide or Wet milling colloidal aluminium oxide (Dispal 'M') and colloidal silicon dioxide (Ludox) in a rubber-lined ball mill for 16 h Commercial mullites	≥ 73·9 wt % aluminium oxide prepared from both methods Between ≃ 72·6 and ≃ 73·6 wt % aluminium oxide prepared from both methods	1650, 1700 or 1750 °C	Mullite and corundum Only mullite	Mainly equiaxed grains A mixture of acicular and polygonal grains Small interlocking acicular grains with a large amount of glassy (intergranular) phase	
30	Hydrolysing a mixture of aluminium tris isopropoxide and silicon tetrakis isopropoxide followed by calcination at 600 °C for 1 h	71·8 wt % aluminium oxide	Fired from 1200–1700 °C Vacuum hot-pressed at 1500 °C for 30 min	Only mullite at any stage Only mullite	A mixture of acicular and polygonal grains	
27	γ-Aluminium oxide (300 Å) and amorphous silicon dioxide (130–140 Å) mixed via a gel technique	71·8 wt % aluminium oxide	Fired at 1420 °C for 20 h	Only mullite	Equiaxed grains	
26	Prepared from pure organo-metallic precursors purified by chemical methods	74·53 and 66·68 wt % aluminium oxide	Heated up to 1500 °C	Mullite and corundum (due to incomplete reaction)		Intensity of mullite peaks in XRD patterns showed more mullite in 74·53 wt % Al_2O_3 mixture
38	α-Aluminium oxide and fused silicon dioxide	70·0 wt % aluminium oxide 75·0 wt % aluminium oxide 77·5 wt % aluminium oxide	Homogenized at 2100 °C for 24 h and slowly cooled to solidification over 13 days	Mullite with 76·7 wt % Al_2O_3 Mullite with 77·2 wt % Al_2O_3 Mullite with 77·8 wt % Al_2O_3	Bundles of acicular mullite needles in a glassy matrix	
39	α-Aluminium oxide (XA16-ALCOA) and fused silica (Corning 7940)	60·0 wt % aluminium oxide	Homogenized at 2090 °C for 55 min Quenched to room temperature Undercooled to 1725 °C; held for 1·5 h; quenched After quenching to room temperature, reheated at 1725 °C for 70 h	Mullite with 78·4 wt % Al_2O_3 Mullite with 74·5 wt % Al_2O_3	Long mullite needles (≃ 20 × 250 μm) in a glassy phase having 18·5 wt % Al_2O_3 Mullite needles of larger section (≫ 20 μm) in a glassy phase having 23·5 wt % Al_2O_3	When homogenized melt was quenched to room temperature and reheated at 1725 °C, initial mullite needles (≃ 20 × 250 μm) recrystallized and grew in section while the Al_2O_3 content of the liquid phase increased from 18·5 to 23·5 wt % Al_2O_3 due to exsolution of Al_2O_3 from mullite, changing its composition from 78·4 to 74·5 wt % Al_2O_3

TABLE 3
Influence of Additives on Synthesis of Mullite

Reference	*Additive*	*Solubility of additive in mullite*	*Effect of additive on:*			*Other remarks*
			Mullite lattice parameters	*Mullitization*	*Mullite grain growth*	
32	Fe_2O_3	< 5 wt% at 1200 °C, 10–12 wt% at 1300 °C	All lattice parameters increase with Fe_2O_3 content in solid solution			
	Cr_2O_3	Negligible at 1200 °C, 8–12 wt% at 1600 °C	All lattice parameters increase with Cr_2O_3 content in solid solution			
	TiO_2	Negligible at 1200 °C, 2–4 wt% at 1600 °C	All lattice parameters increase with TiO_2 content in solid solution			
29	Fe_2O_3	≃ 12 wt% at 1300 °C	Cell volume increases with Fe_2O_3 content in solid solution	Lowers the mullitization temperature; enhances mullitization	Increases the rate of grain growth	All mixtures were studied in the temperature range 900–1500 °C and contained 3–12 wt% additive
	TiO_2	≃ 3 wt% above 1300 °C	Cell volume increases with TiO_2 content in solid solution	Enhances mullitization (effect is less than that of Fe_2O_3)	Inhibits grain growth	
45	Fe_2O_3	7·7 wt% at 1300 °C				Refractive index increases and XRD lines shift with Fe_2O_3 content in solid solution
	FeO	Not soluble				FeO reacts with mullite at ≃ 1190 °C to give $FeAl_2O_4$ and Fe_2SiO_4

43	Fe_2O_3	High		Increases the rate of grain growth	All mixtures were studied in the temperature range 1650–1700 °C; Fe_2O_3 changes the morphology of mullite from 'rectangular with rounded ends' to 'acicular'
	TiO_2	Low		Increases the rate of grain growth (effect is less than that of Fe_2O_3	
	CaO	Very low		Increases the rate of grain growth (effect is more than that of Fe_2O_3	
	K_2O, Na_2O			No effect	
46	Fe_2O_3		Enhances mullitization when <5 mol % added		All mixtures were fired at 1200 °C for 9 h; presence of K_2O and Na_2O diminishes the effect of Fe_2O_3 and TiO_2; the effect of TiO_2 depends on the Al_2O_3/SiO_2 ratio of the mixtures
	TiO_2		Enhances mullitization (effect is less than that of Fe_2O_3)		
	Na_2O, K_2O		No effect		
44	TiO_2	Not more than 3 wt % at any temperature		Increases grain growth (0·3 μm without TiO_2; 2·0 μm with 3 wt % TiO_2, when fired at 1600 °C for 1 h)	Presence of TiO_2 in excess of solubility limit (i.e. >3 wt %) decreases the rate of sintering, probably due to the precipitation of Al_2TiO_5 at the grain boundaries
42	Ba^{2+}, Ca^{2+}, Be^{2+}		Enhances mullitization		All mixtures were studied at 1350 °C; Ba^{2+}, Ca^{2+} and Be^{2+} increase the amount of mullite formed from 53 % to 91, 88 and 75 %, respectively, while Fe^{3+} and Ni^{3+} decrease mullitization by 46 and 40 %, respectively
	B^{3+}, Ti^{4+}, Zr^{4+}, Mn^{4+}, Mg^{2+}		No effect		
	Fe^{3+}, Ni^{3+}		Diminishes mullitization		
40	ZrO_2	Very low ($0·5 \pm 0·1$ wt %)			
41	ZrO_2	$\simeq 35$ wt % ZrO_2			

Moya and Osendi,[40] is probable, but a very high solubility of zirconium dioxide in mullite, as reported by Dinger *et al.*,[41] remains to be confirmed.

Despite the contradictory observation of Budnikov *et al.*,[42] who found a decrease of mullitization of aluminium oxide/silicon dioxide mixtures in the presence of Fe^{3+}, it generally appears that iron(III) oxide, titanium dioxide and calcium oxide facilitate mullitization of aluminium oxide/silicon dioxide mixtures. Iron(III) oxide favours grain growth and probably leads to a microstructure with large elongated grains, as Johnson and Pask[43] observed. On the other hand, small amounts of alkali-oxides do not appear to have a significant effect on mullitization or grain growth. For other additives, definitive conclusions cannot be drawn because of lack of precise information and/or contradictory observations.

2.3. Sintering of mullite

Although mullite has been the subject of many investigations, few of them have been devoted to the sintering of synthetic mullite. The results of those few studies (Table 4) show that the hot-pressing of very fine powders is required to obtain a full densification at rather low temperatures. For pressureless sintering, treatments at $< 1650\,^{\circ}C$ do not lead to densifications above 95%.

Nearly all the data concerning densification during hot-pressing, grain growth and creep lead to apparent activation enthalpies of about $700\,kJ\,mol^{-1}$. Such a value is very similar to that for lattice diffusion of Si^{4+} ($702\,kJ\,mol^{-1}$),[47] which could mean that the diffusion of silicon ions is the rate-controlling process for densification, grain growth and creep of mullite. Other creep data (stress component between 1·3 and 2,[48] grain size dependence of -2[49]) also support the idea that silicon diffusion plays the main role. However, it should be noted that Sacks and Pask[33] have observed an activation enthalpy of about $305\,kJ\,mol^{-1}$ for the early stages of densification during pressureless sintering.

On the one hand, mullite does not sinter easily and, on the other, high purity mullite powders are not so easily found in the market (compared to silicon dioxide and aluminium oxide powders). This strongly suggests the use of reaction sintering:

$$3Al_2O_3 + 2SiO_2 \rightarrow 3Al_2O_3 \cdot 2SiO_2$$

(for the case of 3:2 'stoichiometric' mullite).

However, it has been observed that the formation of mullite retards densification for α-aluminium oxide–amorphous silicon dioxide mixtures,[23] as well as α-aluminium oxide–quartz and α-aluminium oxide–cristobalite[22] mixtures. This could be linked to the two processes involved in reaction sintering (densification and reaction) which can be simultaneous or not, and

which can be mutually favourable or not. In the case of mullite, the high activation enthalpy of this compound makes it difficult to sinter at low temperatures. Moreover, dilatometric effects ($\rho(3Al_2O_3 + 2SiO_2) \simeq 3{\cdot}31\ Mg\,m^{-3} \rightarrow \rho(\text{mullite}) \simeq 3{\cdot}16\ Mg\,m^{-3}$) can disturb the densification mechanisms.

Hence it would seem better to densify before the mullitization, which could be done by varying one or more of the parameters involved in reaction sintering, such as the crystalline form of reactants, particle size, firing temperature and time. Particle size would seem the best parameter, as pointed out by Brook and Yangyun[50] in a general paper on reaction sintering: the densification kinetics depend on D^{-2} or D^{-3} (D being the mean particle size) whereas the reaction kinetics depend on D^{-1} or D^{-2}. Hence densification can be favoured against reaction by decreasing the particle size. This may be the reason why Moya and co-workers[44,51] succeeded in sintering at a fairly low temperature very fine 'premullite' powders (Table 4). However, the effect of the crystalline form of silicon dioxide and aluminium oxide on mullitization should also be employed to delay the reaction (i.e. using the least reactive aluminium oxide and silicon dioxide species). This encourages us to avoid the use of cristobalite and γ-aluminium oxide which favours the reaction, and to choose amorphous silicon dioxide and α-aluminium oxide with the complementary advantages that both materials are common ceramic raw materials and can be found in a wide range of grades, and that α-aluminium oxide has better compaction properties and a lower firing shrinkage than γ-aluminium oxide.

3. EXPERIMENTAL PROCEDURE

3.1. Preparation and sintering of specimens

The raw materials used were α-aluminium oxide* and amorphous silicon dioxide†. The powder mixtures were prepared by attrition milling in ethanol, using zirconia balls as the grinding media. The mill liner was of hardened steel. The iron introduced by grinding for 3 h (0·025 % Fe_2O_3) is less than the iron impurity in the aluminium oxide powder (0·03 %).

After drying, crushing and passing through a 200 μm sieve, the powder mixtures were mixed with 3 wt % polymethylmethacrylate dissolved in

*RC-172 DBM, Reynolds Metals Company, Chemical Division, Arkansas; chemical analysis (wt %): 0·05 Na_2O, 0·07 SiO_2, 0·03 Fe_2O_3 and 0·07 CaO; mean particle size $\simeq 0{\cdot}64\ \mu m$.

† Alfa 89709 silicon(IV) oxide, <400 mesh powder (mean particle size $\simeq 3{\cdot}6\ \mu m$); Alfa Research Chemicals and Materials, 7500 Karlsruhe; impurity content is $<0{\cdot}5$ wt %.

TABLE 4
Sintering of Mullite

Reference	*Preparation of mullite*	*Composition* ($wt\%$ Al_2O_3)	*Sintering conditions*	*Porosity* (%)	*Activation enthalpy/kJ mol*$^{-1}$			*Other remarks*
					Sintering	*Grain growth*	*Creep*	
30	Derived from corresponding metal alkoxides	71·8	Vacuum hot-pressing at 1500 °C for 30 min	< 1				Before processing, as-prepared $3Al_2O_3 \cdot 2SiO_2$ powder, calcined at 600 °C for 1 h (specific surface $\simeq 280\,m^2\,g^{-1}$), was ground in a boron carbide mortar
49	Same as for Ref. 30	71·8	Vacuum hot-pressing at 1500 °C for 30 min	< 1			≃711	Grain size dependence of steady-state creep rate at 1400 °C was found to be -2
48	γ-Aluminium oxide (300 Å) and amorphous silicon dioxide (130–140 Å), mixed via a gel technique, was fired for 20 h at 1420 °C; surface area of mullite obtained was approximately $5{\cdot}5\,m^2\,g^{-1}$	71·8	Hot-pressed between 1470 and 1620 °C and ≃7 to ≃42 MPa	≃1·7 and ≃1·3 for hot-pressing at 1580 and 1620 °C	681 ± 92	761 ± 188		Stress component for creep was found to be 1·3–2·0
54	Same as for Ref. 48	71·8	Hot-pressed between 1450 and 1650 °C and ≃14 to ≃35 MPa	Minimum porosity was ≃5	706 ± 63			Stress component for creep was found to be 1·41 ± 0·65
28	Aluminium oxide and silicon dioxide of colloidal particle size mixed and milled in a rubber-lined ball mill, dried and calcined at 1560 °C for 3 h gave only mullite; it was ground for 6–114 h and all particles > 4 μm were removed	≃71·8	1 h at ≃1700 °C	2–3				Specimens were prepared by cold pressing under ≃155 MPa
	Aluminium oxide silicon dioxide mixtures obtained by hydrolysing tetraethyl silicate in the presence of aluminium hydroxide and calcined at 1400 °C for 4 h gave only mullite; it was wet or dry milled before agglomerating for cold pressing	≃71·8	1–4 h at 1650 °C 1–4 h at 1700 °C 1–4 h at 1750 °C	≃14 ≃3 ≃3				

33	Mixtures of A14-ALCOA (α-aluminium oxide) and α-quartz wet mixed in isopropanol in a porcelain ball mill, calcined at 1700 °C for 8 h, were crushed in a mechanically operated mortar and pestle and wet ground in a vibratory mill for 5 h	71·8 73·0 74·0	1 h 4 h 12 h } at 1700 °C	≃20 ≃13 ≃5·5	≃305 for early stages of sintering	Similar results were obtained using mullites prepared from two other processes; about 97% dense mullite was obtained from mullite powders ground for 36 h; specimens were die-formed under uniaxial pressure (17 MPa) followed by isostatically pressing at 170 MPa
52	α-Aluminium oxide (A16-ALCOA) and silicon dioxide (precipitated silica) milled in a plastic bottle for 2 h in methylated spirits with alumina balls was calcined and ground again for 1 h as above	71·8	2 h at { 1550 °C 1575 °C 1650 °C	16·6 11·8–14·4 9·6		Specimens were prepared by double-ended cold pressing under 70 MPa
53	Mixture of $Al(NO_3)_3 \cdot 9H_2O$ and silicon dioxide (Corning 9604) reactive fired for 24 h at 1600 °C was pulverized for 4 h in a vibrating mill using agate or alumina balls and ethanol: the slurry was dried and screened (average particle size ≃2 μm)	71·8	20 h at 1800 °C	≃7		Specimens (7–10 mm high, 6·4 mm in diameter) were obtained by uniaxial pressing at ≃120 MPa
36	Mixture of aluminium nitrate and tetraethyl silicate dissolved in water–methanol (1:1 by volume) sprayed into a preheated (650 °C) quartz reaction tube, calcined at 1000 °C for 1 h and ground in a vibrating mill for 50 h	71·8	4 h at 1650 °C	≃5		Surface area of as-prepared powder (≃15 $m^2 g^{-1}$) decreased down to ≃2 $m^2 g^{-1}$ when calcined at 1000 °C for 1 h; specimens were prepared by rubber pressing under 200 MPa
51	Al_2O_3–SiO_2 mixture of amorphous nature (called premullite) obtained by thermal and chemical treatment of a kandite (surface area ≃250 $m^2 g^{-1}$); powder was attrition milled for 1 h	72·2	2·5 h at 1570 °C	3·0		A considerable amount of impurities (e.g. CaO ≃0·2 wt%, Fe_2O_3 ≃0·15 wt%) were present in the prepared mullite; mullite formation begins at a temperature between 1200 and 1350 °C
44	Same as for Ref. 51	72·2	1–16 h at 1600 °C	≃5·0		Specimens were prepared by isostatically pressing under 200 MPa

diethyl ether (1 g in 100 ml) for 30 min and dried on a hot plate while mixed continuously. After evaporating the ether, the powder mixtures were de-agglomerated by crushing and passing through a 200 μm sieve. Specimens in the form of discs (30 mm diameter, 3–5 mm thickness) were obtained by cold pressing under $\simeq 150$ MPa in a floating steel die, using a simple hydraulic press. To obtain a better compaction and to minimize defects[55] the lower piston of the pressing assembly was subjected to an ultrasonic vibration (frequency = 20 kHz, amplitude = 10 μm) during the first 3 s of pressing.

Specimens were sintered in an electric furnace of low thermal inertia. The organic binder was burned off by heating at a low rate of $\simeq 15\,^{\circ}\mathrm{C\ min^{-1}}$ up to 800 °C and then heated at a rate of $\simeq 60\,^{\circ}\mathrm{C\ min^{-1}}$ up to the soaking temperature. After a given heat treatment the specimens were allowed to cool naturally in the furnace.

3.2. Characterization of the sintered specimens

The bulk density was determined using the liquid displacement technique with distilled water as the liquid media.

Microstructural observations were done on polished and thermally etched specimens using a JEOL T200 scanning electron microscope. Thermal etching time varied from 20 to 30 min depending on the etching temperature, which was always 100 °C less than the sintering temperature.

Both qualitative and quantitative analyses of the crystalline phases of the fired specimens were carried out using their X-ray diffraction (XRD) (Cu-Kα) patterns. The peaks used, corresponding to different phases, are given in Table 5.

S_M, S_C, S_A and S_{A^*} represent the areas under the respective peaks. Plots of $S_A/(S_M + S_A)$ or $S_{A^*}/(S_M + S_{A^*})$ versus α-aluminium oxide wt% for α-aluminium oxide–mullite mixtures and a plot of $S_C/(S_M + S_C)$ versus

TABLE 5
X-ray Diffraction Peaks of Different Phases Used for Quantitative Analysis

Crystalline phase	*Indices of the corresponding atomic plane*	*2θ value in Cu-Kα XRD pattern deg*	*Relative peak intensity*	*Interplanar distance* A	*Symbol*
Mullite	(210)	26·26	100	3·39	M
β-Cristobalite	(101)	21·92	100	4·05	C
α-Aluminium oxide	(113)	43·24	100	2·09	A
	(012)	25·58	70	3·48	A*

β-cristobalite wt % for β-cristobalite–mullite mixtures were constructed using XRD patterns of two series of mechanical mixtures. Mullite obtained by firing an amorphous silicon dioxide–α-aluminium oxide mixture of 71·8 wt % Al_2O_3 for 10 h at 1650 °C, β-cristobalite obtained by firing amorphous silicon dioxide for 10 h at 1600 °C and as-received α-aluminium oxide were used for preparing mechanical mixtures. The amount of free α-aluminium oxide or of free β-cristobalite present in fired specimens was determined using the $S_A/(S_M + S_A)$, $S_{A^*}/(S_M + S_{A^*})$ and $S_C/(S_M + S_C)$ ratios of the corresponding XRD patterns and the three plots constructed as explained above.

3.3. Results and discussion

3.3.1. Effects of the particle size of powders on the reactions and on the shrinkage behaviour

Powder mixtures of 71·8 wt % aluminium oxide composition attrition milled for 0, 1 and 5 h were used for this study. The dilatometric shrinkage curves (Fig. 2) were obtained using rectangular bars (4 × 4 × 20 mm) cut from pressed discs. The curves consist of a number of zones, which become more distinct with the increase of milling time. The sintering process is affected by

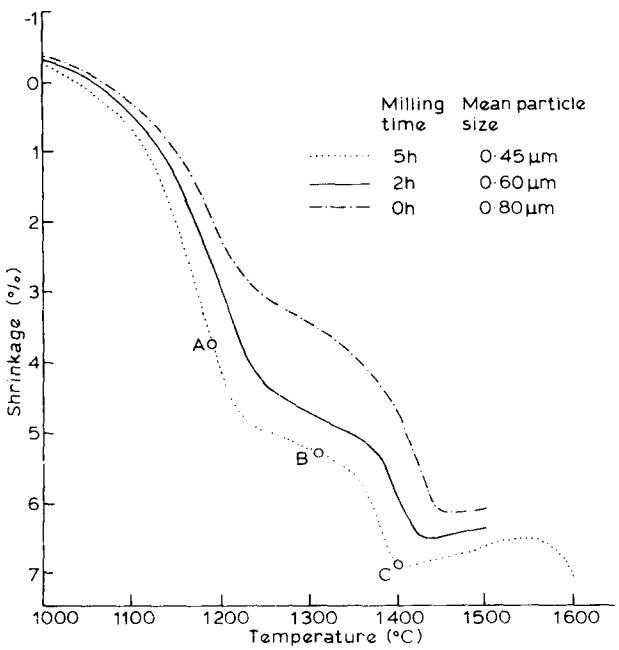

Fig. 2. Percentage shrinkage versus temperature for mixtures of 71·8 wt % aluminium oxide composition and different fineness.

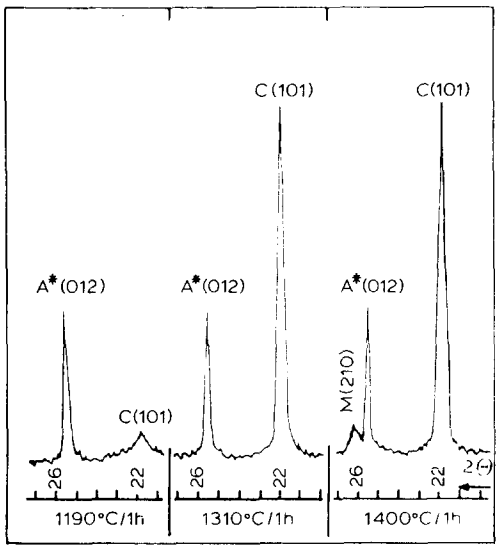

Fig. 3. X-ray diffraction patterns of 5 h attrition milled 71·8 wt % aluminium oxide mixture, fired under different conditions as indicated.

two phenomena, one taking place in a range of temperatures around 1300 °C and the other just above 1400 °C. To understand these phenomena, the mixture attrition milled for 5 h was studied further. Three samples of this mixture were fired for 1 h at 1190, 1310 and 1400 °C, the temperatures corresponding to the three points A, B and C marked on the corresponding shrinkage curve. After firing, they were analysed by X-ray diffraction. The observed XRD patterns are given in Fig. 3. At 1190 °C the most intense peak of cristobalite (C(101)) starts to appear and at 1310 °C it is of high intensity. The value of $S_C/(S_C + S_{A^*})$ is the same for XRD patterns corresponding to the specimens fired at 1310 and 1400 °C, which means that the cristobalite/aluminium oxide ratio remains almost constant from 1310 °C. At 1400 °C the (210) peak of mullite begins to develop. At any temperature above 1400 °C mullite develops at the expense of α-aluminium oxide and cristobalite. The following conclusions can be drawn from these observations:

1. Transformation of amorphous silicon dioxide into cristobalite takes place in the temperature range where the first sudden change in the rate of shrinkage is observed, and is almost complete before the beginning of the mullite formation.
2. The mullite formation starts just before the second sudden change in the rate of shrinkage and it causes a net overall expansion of the body.

The transformation of amorphous silicon dioxide (density $\simeq$ 2·22 Mg m^{-3}) into cristobalite (density $\simeq$ 2·32 Mg m^{-3}) is accompanied by a decrease of the rate of shrinkage, which is contrary to what would be expected for such a transformation, where a low-density phase transforms into a higher density phase. One possible reason for this behaviour is the formation of microflaws caused by a sudden contraction of silicon dioxide zones, which leads to a reduction of the number of particle-to-particle contacts. Another possible reason is the elimination of the amorphous phase (amorphous silicon dioxide), which may have helped densification at lower temperatures by acting as an easy diffusion path. The rapid rate of shrinkage just before the appearance of mullite (i.e. after the amorphous silicon dioxide → cristobalite transformation) may be due to the formation of a metastable liquid phase in accordance with the α-aluminium oxide–cristobalite metastable equilibrium diagram in the absence of mullite (Fig. 1).

By comparing these shrinkage curves, it can be seen that the reduction of particle size has caused an increase in the total shrinkage before mullitization, in addition to a slight reduction of the mullitization temperature. This shows the beneficial influence, for sintering, of using fine powders, as has been pointed out by Brook and Yangyun.[50] Hence, it may be possible to use the particle size effect to improve the densification before mullitization, during reaction sintering of aluminium oxide–silicon dioxide mixtures, thereby reducing the difficulty in sintering caused by the mullite formation.

3.3.2. Effect of composition on reaction, densification and microstructure

The effects of the composition on reaction and densification were investigated using five different compositions, namely 68·0, 71·8, 75·0, 77·3 and 80·0 wt % aluminium oxide, prepared by attrition milling for 3 h. The powder compacts were subjected to three different heat treatments (10 and 2 h at 1600 °C and 2 h at 1570 °C). The results of the experiments are given in Tables 6 and 7 and Figs 4a, 4b, 5 and 6. Although the results concerning specimens fired at 1570 °C for 2 h are given in Table 7 and Fig. 5, they are not discussed herein due to the difficulty of interpretation caused by incomplete reaction.

X-ray diffraction patterns given in Figs 4a and 4b correspond to the specimens fired at 1600 °C for 2 and 10 h, respectively. In both groups of XRD patterns, the compositions with 68·0 and 71·8 wt % Al_2O_3 do not show the presence of any crystalline phase other than mullite, but for the compositions with 75·0, 77·3 and 80·0 wt % Al_2O_3 the peaks of α-aluminium oxide can be seen. Their intensities show that the highest amount of free α-aluminium oxide is in the specimen with 80·0 wt % Al_2O_3 and the lowest

TABLE 6

Bulk Density and Relative Densification of α-Aluminium Oxide–Amorphous Silicon Dioxide Mixtures of Different Compositions, Fired Under Different Conditions

Composition (wt% aluminium oxide)	*Bulk density of the green compacts / Mg m⁻³ (% compaction)*	*2 h at 1570°C*		*2 h at 1600°C*		*10 h at 1600°C*	
		Density / Mg m⁻³	*Densification / %*	*Density / Mg m⁻³*	*Densification / %*	*Density / Mg m⁻³*	*Densification / %*
68·0	1·85 (58·3)	2·78	90·0	2·83	91·6	2·95	95·5
71·8	1·90 (58·4)	2·90	91·8	2·95	93·4	3·07	97·2
75·0	1·94 (58·4)	2·85	88·4	2·91	90·2	3·01	93·3
77·3	1·97 (58·4)	2·94	89·6	2·99	91·2	3·11	94·8
80·0	2·00 (58·2)	3·07	91·6	3·15	94·0	3·23	96·4

TABLE 7

Composition of Mullite Solid Solution in α-Al_2O_3–Amorphous Silicon Dioxide Mixtures of Different Al_2O_3/SiO_2 Ratios Fired at 1600 °C for 10 h

Composition of the mixture (wt% aluminium oxide)	*Estimated free α-aluminium oxide content (wt%)*	*Combined Al_2O_3 content (wt%)*	*Composition of mullite solid solution*[a] *(wt% Al_2O_3)*	*Free silicon dioxide content (wt%)*	*Theoretical density ($Mg\,m^{-3}$)*
68·0	—	68·0	71·8	5·3	3·09
71·8	—	71·8	71·8	—	3·16
75·0	1·0	74·0	74·7	—	3·225
77·3	10·0	67·3	74·8	—	3·28
80·0	20·5	59·5	74·8	—	3·35

[a] It was considered that the silicon dioxide-rich end of the mullite solid solution is 71·8 wt% Al_2O_3.

one in the specimen with 75·0 wt% Al_2O_3. This XRD observation is confirmed by the corresponding micrographs (Fig. 6): a noticeable amount of free α-aluminium oxide (white grains) in the 80·0 wt% Al_2O_3 specimen and a very low amount of free α-aluminium oxide (a few very small white grains, both at intergranular and intragranular positions) in the 75·0 wt% Al_2O_3 specimen.

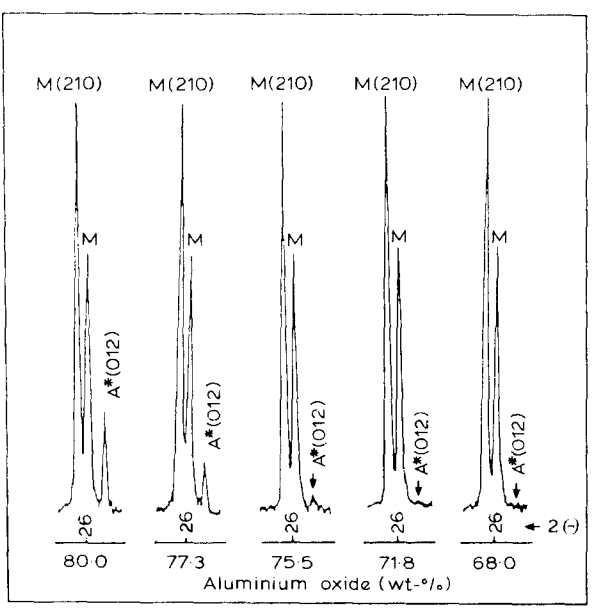

Fig. 4a. X-ray diffraction patterns (around the (210) mullite peak) of mixtures of various indicated aluminium oxide/silicon dioxide ratios fired for 2 h at 1600 °C.

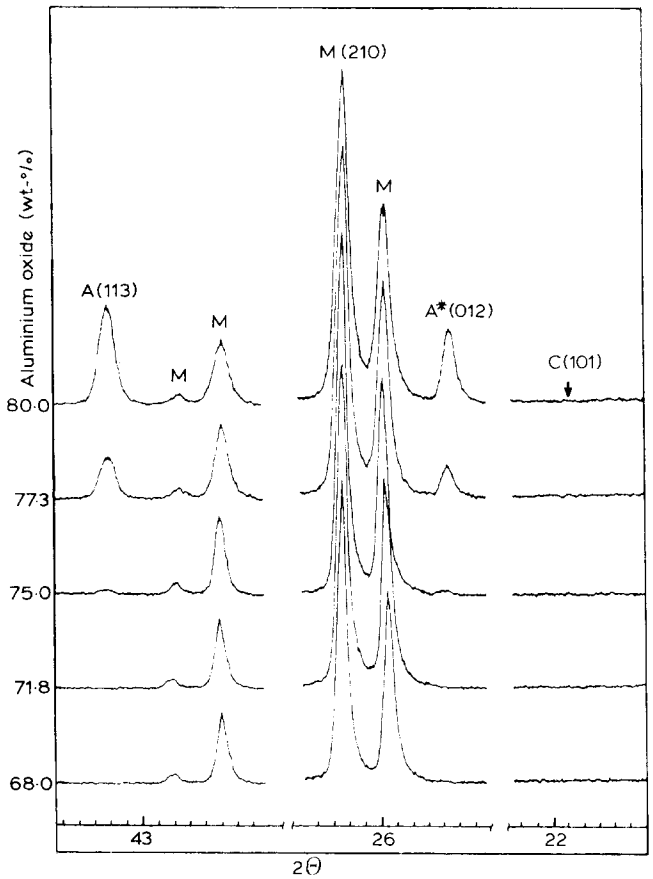

Fig. 4b. X-ray diffraction patterns of mixtures of various indicated aluminium oxide/silicon dioxide ratios fired for 10 h at 1600 °C.

Results of the quantitative estimations of free α-aluminium oxide in the specimens fired at 1600 °C for 10 h are given in Table 7. Similar results were obtained for specimens fired at 1600 °C for 2 h (see the similarity of XRD patterns in Figs 4a and 4b). Hence, mullitization has ended even before 2 h at 1600 °C.

If only α-aluminium oxide and mullite are present in fired 75·0, 77·3 and 80·0 wt % Al_2O_3 specimens, as evidenced by corresponding XRD patterns and micrographs, the composition of mullite in those specimens can be determined using the estimated values of free α-aluminium oxide (Table 7, column 2). It shows that the composition of the mullite solid solution remains constant at $\simeq 74{\cdot}8$ wt % and is independent of the original composition for mixtures having $\geq 75{\cdot}0$ wt % Al_2O_3. Consequently, the aluminium oxide-rich end of the mullite solid solution is limited to

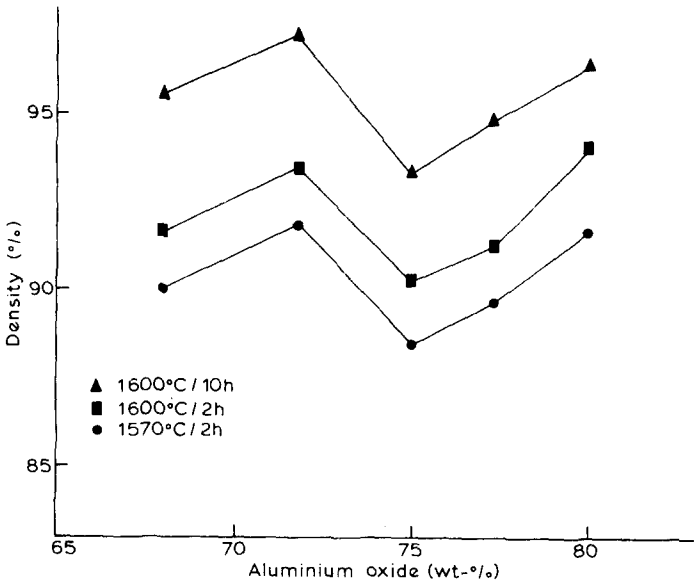

Fig. 5. Percentage density versus aluminium oxide content for α-aluminium oxide–amorphous silicon dioxide compacts fired under different conditions as indicated.

$\simeq 74{\cdot}8$ wt % Al_2O_3. This is slightly higher than the corresponding values obtained by Aramaki and Roy[2] and Aksay and Pask.[13]

If the silicon dioxide-rich end of the mullite solid solution is 71·8 wt % Al_2O_3 (as proposed by Aramaki and Roy) or 70·5 wt % Al_2O_3 (as proposed by Aksay and Pask), the fired 68·0 wt % Al_2O_3 specimen should contain $\simeq 5{\cdot}3$ or $\simeq 3{\cdot}5$ wt % free silicon dioxide, respectively. But no crystalline silicon dioxide was found in 71·8 and 68·0 wt % Al_2O_3 mixtures. However, this does not mean that the silicon dioxide-rich end of the mullite solid solution is below 68·0 wt % Al_2O_3, since, unlike free aluminium oxide, free silicon dioxide can be present as a vitreous phase. Hence no conclusion about the silicon dioxide-rich end of the mullite solid solution can be drawn without separating and analysing mullite in the fired 71·8 and 68·0 wt % Al_2O_3 specimens.

To determine the extent of densification, the theoretical density of each fired composition was calculated under the following assumptions:

1. The range of the mullite solid solution is from 71·8 to 74·8 wt % Al_2O_3, while its density varies from 3·16 to 3·22 Mg m^{-3}.
2. Excess aluminium oxide is present in the form of α-aluminium oxide (density = 3·98 Mg m^{-3}) whereas excess silicon dioxide is present in the form of a vitreous phase. The density of the latter was considered to be similar to that of the amorphous silica used (2·22 Mg m^{-3}).

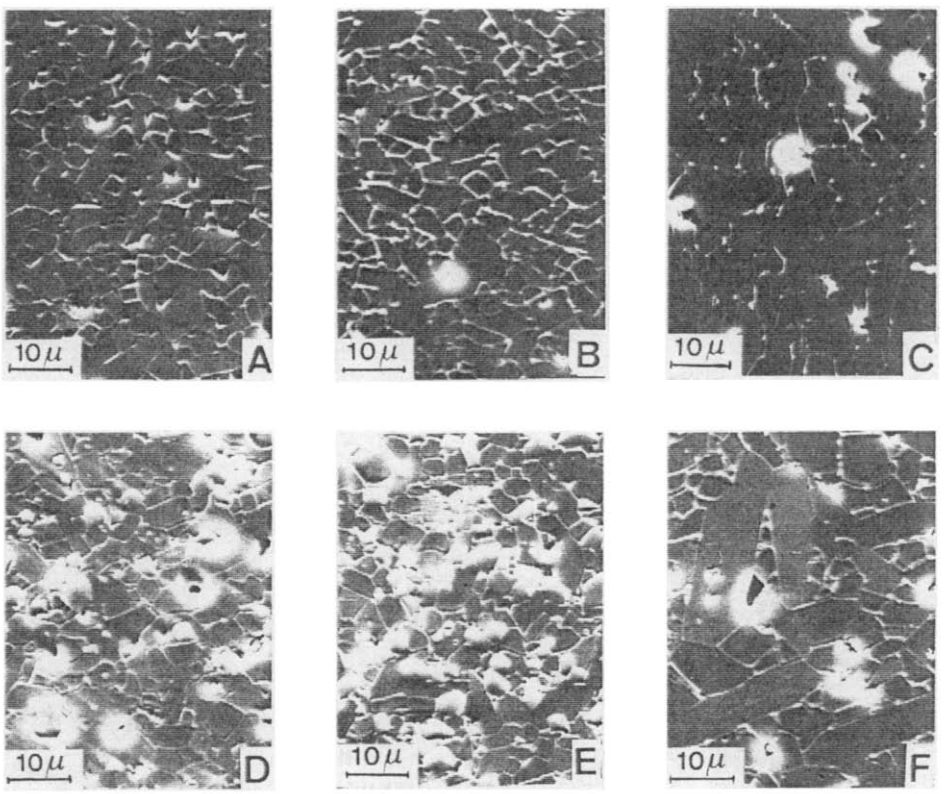

Fig. 6. Microstructures of (A) 68·0, (B) 71·8, (C) 75·0, (D) 77·3, (E) 80·0 and (F) 75·0 wt % Al_2O_3 compositions, fired 10 h at 1600 °C (thermal etching: 20 min at 1500 °C).

The bulk density and the percentage densification of each composition after each heat treatment are given in Table 6. Figure 5 shows that the densification versus wt % Al_2O_3 plots consist of maxima at 71·8 wt % Al_2O_3 and minima at 75·0 wt % Al_2O_3. This is confirmed by the micrographs in Fig. 6. The lower densification of the 75·0 wt % Al_2O_3 composition is coupled with a higher rate of grain growth, leading to a microstructure which consists of a mixture of large elongated grains ($\simeq 7 \times 30\ \mu m$) with small equiaxed grains ($\simeq 5 \times 5\ \mu m$), whereas the microstructures of the other compositions are more or less equiaxed. This peculiar behaviour of the 75·0 wt % Al_2O_3 composition is not yet understood and is being studied further.

4. CONCLUSIONS

This paper shows that the reaction sintering of amorphous silicon dioxide–α-aluminium oxide mixtures is a good way of producing high

purity, fine grain, nearly dense mullite ceramics. The comparison with alumina—which is justified by the fact that this material remains the archetype of high technology ceramics—demonstrates that reaction-sintered mullite can be processed using similar treatments as those required by 'reactive' aluminium oxide. Indeed, nearly dense ($\simeq 97\%$), fine grain ($\simeq 5\ \mu m$) mullite is obtained after firing for some hours at 1600 °C, i.e. after a treatment close to that required by RC-172 DBM Reynolds aluminium oxide. However, the particle size of the initial mixture must be as fine as possible, which could call for an additional grinding. The aluminium oxide/silicon dioxide ratio appears to be a critical parameter: the composition of $3Al_2O_3 \cdot 2SiO_2$ stoichiometric mullite ($\simeq 71{\cdot}8$ wt % Al_2O_3) leads to the best densification, and the finest microstructure. On the other hand, compositions near the limit of solubility of Al_2O_3 in mullite ($74{\cdot}8$ wt % Al_2O_3) exhibit rather poor densification and excessive grain growth. Further studies are being done to understand this behaviour.

As far as the mechanical properties are concerned, reaction-sintered stoichiometric mullite has a room-temperature flexure strength of $\simeq 200$ MPa (biaxial flexure on 30 mm diameter discs) and toughness, K_{Ic}, of $\simeq 2{\cdot}2$ MPa $m^{1/2}$ (SENB experiments on $3 \times 3 \times 30$ mm).[56] The influence of temperature is rather moderate and the flexure strength at 900 °C is $\simeq 150$ MPa. Such values can be favourably compared with those obtained in sintered mullite,[52] even if they cannot compete with zirconium dioxide-toughened mullite.[57,58]

The use of additives, which can lead to vitreous phases which decrease the sintering temperature and which increase the room-temperature strength,[59] is another point requiring further study.

REFERENCES

1. Bowen, N. L. and Greig, J. W., The system Al_2O_3–SiO_2, *J. Am. Ceram. Soc.*, **7** (1924) 238.
2. Aramaki, S. and Roy, R., Revised phase diagram for the system Al_2O_3–SiO_2, *J. Am. Ceram. Soc.*, **45** (1962) 229.
3. Rooksby, H. P. and Partridge, J. H., X-ray study of natural and artificial mullites, *J. Soc. Glass Technol.*, **23** (1939) 338T.
4. Bárta, R. and Bárta, C., A study of the system Al_2O_3–SiO_2, *Zh. Priklad Khim.*, **29** (1956) 341.
5. Neuhaus, A. and Richartz, W., Über die Einkristallzuchtung und Zustandsverhaltniss von Mullit [Growing of single crystals of mullite and their constitution], *Ber. Deut. Keram. Ges.*, **35** (1958) 108.
6. Welch, J. H., A new interpretation of the mullite problem, *Nature*, **186** (1960) 545.

7. Bauer, W. H., Gordon, I. and Moore, C. H., Flame fusion synthesis of mullite single crystals, *J. Am. Ceram. Soc.*, **33** (1950) 140.
8. Toropov, N. A. and Galakhov, F. Y., New data for the system Al_2O_3–SiO_2, *Dokl. Akad. Nauk SSSR*, **78** (1951) 299.
9. Trömel, G., Comments on the equilibrium diagram Al_2O_3–SiO_2, in *Conference on Physical Chemistry of Iron and Steel Making*, MIT Press, Cambridge, Mass., 1956, 77–8.
10. Filonenko, N. E. and Lavrov, I. V., Fusion of mullite, *Dokl. Akad. Nauk SSSR*, **89** (1953) 141.
11. Trömel, G., Obst, K. H., Konopicky, K., Bauer, H. and Patzak, I., Untersuchungen im System SiO_2–Al_2O_3 [Investigation in the system SiO_2–Al_2O_3], *Ber. Deut. Keram. Ges.*, **34** (1957) 397.
12. Horibe, T. and Kuwabara, S., Thermo-analytical investigation of phase equilibria in the Al_2O_3–SiO_2 system, *Bull. Chem. Soc. Japan*, **40** (1967) 972.
13. Aksay, I. A. and Pask, J. A., Stable and metastable equilibria in the system SiO_2–Al_2O_3, *J. Am. Ceram. Soc.*, **58** (1975) 507.
14. Aramaki, S. and Roy, R., Revised equilibrium diagram for the system Al_2O_3–SiO_2, *Nature*, **184** (1959) 631.
15. Davis, R. F. and Pask, J. A., Diffusion and reaction studies in the system Al_2O_3–SiO_2, *J. Am. Ceram. Soc.*, **55** (1972) 525.
16. Aksay, I. A. and Pask, J. A., Diffusion in SiO_2–Al_2O_3 melts; for abstract see *Am. Ceram. Soc. Bull.*, **52** (1973) 710.
17. Aksay, I. A., Davis, R. F. and Pask, J. A., Diffusion in mullite ($3Al_2O_3 \cdot 2SiO_2$); for abstract see *Am. Ceram. Soc. Bull.*, **52** (1973) 710.
18. Schneider, S. J. and McDaniel, C. L., Effect of environment upon the melting point of Al_2O_3, *J. Res. Natl. Bur. Stand., Sect. A*, **71** (1967) 317.
19. Greig, J. W., Immiscibility in silicate melts: Part I, *Am. J. Sci.*, **13** (1927) 1; Part II, ibid. 133.
20. Schairer, J. F. and Bowen, N. L., The system K_2O–Al_2O_3–SiO_2, *Am. J. Sci.*, **253** (1955) 681.
21. Wahl, F. M., Grim, R. E. and Graf, R. B., Phase transformation in silica alumina mixtures as examined by continuous x-ray diffraction, *Am. Mineralogist*, **46** (1961) 1064.
22. Rana, A. P. S., Aiko, O. and Pask, J. A., Sintering of α-Al_2O_3/quartz, and α-Al_2O_3/cristobalite related to mullite formation, *Ceram. Int.*, **8** (1982) 151.
23. Nurishi, Y. and Pask, J. A., Sintering of α-Al_2O_3–amorphous silica compacts, *Ceram. Int.*, **8** (1982) 57.
24. Staley, W. G. and Brindley, G. W., Development of noncrystalline material in subsolidus reaction between silica and alumina, *J. Am. Ceram. Soc.*, **52** (1969) 616.
25. DeKeyser, W. L., Reactions at the point of contact between SiO_2 and Al_2O_3, in *Science of Ceramics*, Vol. II, Ed. G. H. Stewart, Academic Press, New York, 1963, 243–57.
26. West, R. R. and Gray, T. J., Reactions in silica–alumina mixtures, *J. Am. Ceram. Soc.*, **41** (1958) 132.
27. Ghate, B. B., Hasselman, D. P. H. and Spriggs, R. M., Synthesis and characterization of high purity, fine grained mullite, *Bull. Am. Ceram. Soc.*, **52** (1973) 670.
28. Metcalee, B. L. and Sant, J. H., The synthesis, microstructure and physical properties of high purity mullite, *J. Brit. Ceram. Soc.*, **74** (1975) 193.

29. McGee, T. D. and Wirkus, C. D., Mullitization of alumino-silicate gels, *Bull. Am. Ceram. Soc.*, **51** (1972) 577.
30. Mazdiyasni, K. S. and Brown, L. M., Synthesis and mechanical properties of stoichiometric aluminium silicate (mullite), *J. Am. Ceram. Soc.*, **55** (1972) 548.
31. Crofts, J. D. and Marshall, W. W., A novel synthesis of alumino-silicates and similar materials, *Trans. Brit. Ceram. Soc.*, **66** (1967) 121.
32. Murthy, M. K. and Hummel, F. A., X-ray study of the solid solution of TiO_2, Fe_2O_3, and Cr_2O_3 in mullite ($3Al_2O_3 \cdot 2SiO_2$), *J. Am. Ceram. Soc.*, **43** (1960) 267.
33. Sacks, M. D. and Pask, J. A., Sintering of mullite, in *Processing of Crystalline Ceramics, Materials Science Research, Volume II*, Eds Hayne Palmour III, R. F. Davis and T. M. Hare, Plenum Press, New York, 1978, 193–203.
34. Fenstermacher, J. E. and Hummel, F. A., High-temperature mechanical properties of ceramic materials: IV, sintered mullite bodies, *J. Am. Ceram. Soc.*, **44** (1961) 284.
35. Pankratz, L. B., Weller, W. W. and Kelley, K. K., *Low-temperature Heat-content of Mullite*, US Bur. Mines, Rept. Invest., 6287, 1963.
36. Kanzaki, S., Tabata, H., Kumazawa, T. and Ohta, S., Sintering and mechanical properties of stoichiometric mullite, *J. Am. Ceram. Soc.*, **68** (1985) C-6.
37. DeKeyser, W. L., Contribution to the study of sillimanite and mullite by x-rays, *Trans. Brit. Ceram. Soc.*, **50** (1951) 349.
38. Kriven, W. M. and Pask, J. A., Solid solution range and microstructures of melt-grown mullite, *J. Am. Ceram. Soc.*, **66** (1983) 649.
39. Risbud, S. H. and Pask, J. A., Mullite crystallization from SiO_2–Al_2O_3 melts, *J. Am. Ceram. Soc.*, **61** (1978) 63.
40. Moya, J. S. and Osendi, M. I., Effect of ZrO_2 (ss) in mullite on the sintering and mechanical properties of mullite/ZrO_2 composites, *J. Mat. Sci. Lett.*, **2** (1983) 599.
41. Dinger, T. R., Krishnan, K. M., Thomas, G., Osendi, M. I. and Moya, J. S., Investigation of ZrO_2/mullite solid solution by energy dispersive x-ray spectroscopy and electron diffraction, *Acta Met.*, **32** (1984) 1601.
42. Budnikov, P. P., Keshishyan, T. N. and Volkova, A. V., Effect of small additions on mullite formation at low temperatures, *Silikaty Okisly Khim. Vys. Temp.*, **1963** (1963) 233.
43. Johnson, S. M. and Pask, J. A., Role of impurities on formation of mullite from kaolinite and Al_2O_3–SiO_2 mixtures, *Bull. Am. Ceram. Soc.*, **61** (1982) 838.
44. Baudin, C. and Moya, J. S., Influence of titanium dioxide on the sintering and microstructural evolution of mullite. *J. Am. Ceram. Soc.*, **67** (1984) C-134.
45. Brownell, W. E., Subsolidus reactions between mullite and iron oxide, *J. Am. Ceram. Soc.*, **41** (1958) 226.
46. Skinner, K. G., Cook, W. H., Potter, R. A. and Palmour, H., Effect of TiO_2, Fe_2O_3, and alkali on mineralogical and physical properties of mullite-type and mullite-forming Al_2O_3–SiO_2 mixtures: I, *J. Am. Ceram. Soc.*, **36** (1953) 349.
47. Aksay, I. A., *Diffusion and Phase Relationship Studies in the Alumina–Silica System*, PhD Thesis, University of California, Berkeley, California, April 1973.
48. Ghate, B. B., Hasselman, D. P. H. and Spriggs, R. M., Kinetics of pressure-sintering and grain-growth of ultra-fine mullite powder, *Ceram. Int.*, **1** (1975) 105.

49. Dokko, P. C., Pask, J. A. and Mazdiyasni, K. S., High-temperature mechanical properties of mullite under compression, *J. Am. Ceram. Soc.*, **60** (1977) 150.
50. Brook, R. J. and Yangyun, S., Preparation of zirconia-toughened ceramics by reaction sintering, private communication, 1984.
51. Moya, J. S. and Osendi, M. I., Microstructure and mechanical properties of mullite/ZrO_2 composites, *J. Mat. Sci.*, **19** (1984) 2909.
52. de Portu, G. and Henney, J. W., The microstructure and mechanical properties of mullite–zirconia composites, *Trans. Brit. Ceram. Soc.*, **83** (1984) 69.
53. Mussler, B. H. and Shafer, W., Preparation and properties of mullite cordierite composites, *Bull. Am. Ceram. Soc.*, **63** (1984) 705.
54. Penty, R. A., Hasselman, D. P. H. and Spriggs, R. M., Pressure sintering kinetics of fine grained mullite by the change in pressure and temperature technique, *Bull. Am. Ceram. Soc.*, **52** (1973) 692.
55. Rogeaux, B. and Boch, P., Influence of an ultrasonic assistance to the powder compaction on the Weibull modulus of sintered alumina, *J. Mat. Sci. Lett.*, **4** (1985) 403.
56. Rodrigo, P. D. D. and Boch, P., *Mullite Ceramics by Reaction Sintering of Alumina–Silica Mixtures*, Internal Report, École Nationale Supérieure de Céramique Industrielle, Limoges, October 1984.
57. Boch, P. and Giry, J. P., Preparation and properties of reaction-sintered mullite zirconia ceramics, *Mat. Sci. Eng.*, **71** (1985) 39.
58. Claussen, N. and Jahn, J., Mechanical properties of sintered, *in situ*-reacted mullite–zirconia composites, *J. Am. Ceram. Soc.*, **63** (1980) 228.
59. Orange, G., Turpin-Launay, D., Goeuriot, P., Fantozzi, G. and Thevenot, F., *Mechanical Behaviour of a Al_2O_3–AlON Composite Ceramic Material (Aluminalon)*, Sci. Ceramics 12, Saint-Vincent, Italy, June 1983, 661–6.

Received 16 May 1985; amended version received and accepted 25 July 1985